Exchange magnetic field torques in YIG/Pt bilayers observed by the spin-Hall magnetoresistance

Vlietstra, N.; Shan, J.; Castel, V.; Ben Youssef, J.; Bauer, G. E. W.; van Wees, B. J.

Published in:
Applied Physics Letters

DOI:
10.1063/1.4813760

Exchange magnetic field torques in YIG/Pt bilayers observed by the spin-Hall magnetoresistance

N. Vlietstra,[1] J. Shan,[1] V. Castel,[1] J. Ben Youssef,[2] G. E. W. Bauer,[3,4] and B. J. van Wees[1]
[1]*Physics of Nanodevices, Zernike Institute for Advanced Materials, University of Groningen, Groningen, The Netherlands*
[2]*Laboratoire de Magnétisme de Bretagne, CNRS, Université de Bretagne Occidentale, Brest, France*
[3]*Kavli Institute of NanoScience, Delft University of Technology, Delft, The Netherlands*
[4]*Institute for Materials Research and WPI-AIMR, Tohoku University, Sendai, Japan*

(Received 1 May 2013; accepted 26 June 2013; published online 15 July 2013)

The effective field torque of an yttrium-iron-garnet (YIG) film on the spin accumulation in an attached platinum (Pt) film is measured by the spin-Hall magnetoresistance (SMR). As a result, the magnetization direction of a ferromagnetic insulating layer can be measured electrically. Experimental transverse and longitudinal resistances are well described by the theoretical model of SMR in terms of the direct and inverse spin-Hall effect, for different Pt thicknesses [3, 4, 8, and 35 nm]. Adopting a spin-Hall angle of Pt $\theta_{SH} = 0.08$, we obtain the spin diffusion length of Pt ($\lambda = 1.1 \pm 0.3$ nm) as well as the real ($G_r = (7 \pm 3) \times 10^{14}\,\Omega^{-1}\mathrm{m}^{-2}$) and imaginary part ($G_i = (5 \pm 3) \times 10^{13}\,\Omega^{-1}\mathrm{m}^{-2}$) of the spin-mixing conductance and their ratio ($G_r/G_i = 16 \pm 4$).
 [http://dx.doi.org/10.1063/1.4813760]

In spintronics, interfaces between magnets and normal metals are important for the creation and detection of spin currents, which is governed by the difference of the electric conductance for spin up and spin down electrons.[1–3] Another important interaction between the electron spins in the magnetic layer and those in the normal metal, that are polarized perpendicular to the magnetization direction, is governed by the spin-mixing conductance $G_{\uparrow\downarrow}$,[4] which is composed of a real part and an imaginary part ($G_{\uparrow\downarrow} = G_r + iG_i$). G_r is associated with the "in-plane" or "Slonczewski" torque along $\vec{m} \times \vec{\mu} \times \vec{m}$,[5–7] where $\vec{m}$ is the direction of the magnetization of the ferromagnetic layer and $\vec{\mu}$ is the polarization of the spin accumulation at the interface. G_i describes an exchange magnetic field that causes precession of the spin accumulation around $\vec{m}$. This "effective-field" torque associated with G_i points towards $\vec{\mu} \times \vec{m}$.

While several experiments succeeded in measuring G_r,[3,4,7–10] G_i is difficult to determine experimentally, mainly because it is usually an order of magnitude smaller than G_r.[4] The recently discovered spin-Hall magnetoresistance (SMR)[11–14] offers the unique possibility to measure G_i for an interface of a normal metal and a magnetic insulator by exposing it to out-of-plane magnetic fields. Althammer *et al.*[15] carried out a quantitative study of the SMR of Yttrium Iron Garnet (YIG)/Platinum (Pt) bilayers. They obtained an estimate of $G_i = 1.1 \times 10^{13}\,\Omega^{-1}\mathrm{m}^{-2}$ by extrapolating the high field Hall resistances to zero magnetic field.[16]

In this paper, we report experiments in which the contribution of G_r and G_i can be controlled by changing the magnetization direction of the YIG layer by an external magnetic field. Thereby either G_r or G_i can be made to dominate the SMR. By fitting the experimental data by the theoretical model for the SMR,[11] the magnitude of G_r, G_i, and the spin diffusion length λ in Pt are determined.

For SMR measurements, Pt Hall bars with thicknesses of 3, 4, 8, and 35 nm were deposited on YIG by dc sputtering.[12] Simultaneously, a reference sample was fabricated on a Si/SiO_2 substrate. The length and width of the Hall bars are 800 μm and 100 μm, respectively. The YIG has a thickness of 200 nm and is grown by liquid phase epitaxy on a single crystal $Gd_3Ga_4O_{12}$ (GGG) substrate.[17] The magnetization of the YIG has an easy-plane anisotropy, with an in-plane coercive field of only 0.06 mT. To saturate the magnetization of the YIG in the out-of-plane direction, a field above the saturation field B_s ($\mu_0 M_s = 0.176$T)[17] has to be applied. All measurements are carried out at room temperature.

The magnetization of the YIG is controlled by sweeping an out-of-plane applied magnetic field with a small intended in-plane component (see insets of Figs. 1(a) and 1(b)). Fig. 1(a) shows out-of-plane magnetic field sweeps for various directions of the in-plane component of B (and thus M), while measuring the transverse resistance (using a current $I = 1$ mA). For fields above the saturation field ($B > B_s$), a linear magnetic field dependence is observed, that can be partly ascribed to the ordinary Hall effect, but its slope is slightly larger, which suggests the presence of another effect (discussed below). Furthermore, extrapolation of the linear regime for the positive and negative saturated fields to $B = 0$ mT, reveals an offset between both regimes, that, as shown below, can be ascribed to G_i. When B is smaller than the saturation field, the observed signal strongly depends on the angle α between the direction of the charge current J_e and the in-plane component of the magnetic field. This α-dependence is not observed for $B > B_s$. The maximum/minimum magnitude of the peak/dip observed in the non-saturated regime exactly follows the SMR behaviour for in-plane magnetic fields.[12,13] By increasing the magnetic field strength, the magnetization of the YIG is tilted out of the plane and less charge current is generated by the inverse spin-Hall effect in the transverse (and also longitudinal) direction, resulting in a decrease in the SMR signal. The sharp peak

observed around zero applied field can be explained by the reorientation of M in the film plane when B is swept through the coercive field of the YIG.

The corresponding measurements of the longitudinal resistance are shown in Fig. 1(b) (for current $I = 1 - 100\,\mu$A). In this configuration, the signal for $B > B_s$ does not show a field dependence nor an offset between positive and negative field regimes when linearly extrapolated to zero field.

The observed features for the transverse (Fig. 1(a)) as well as the longitudinal (Fig. 1(b)) resistance can be described by the following equations:[11]

$$\rho_T = \Delta\rho_1 m_x m_y + \Delta\rho_2 m_z + (\Delta\rho_{Hall} + \Delta\rho_{add})B_z, \quad (1)$$

$$\rho_L = \rho + \Delta\rho_0 + \Delta\rho_1(1 - m_y^2), \quad (2)$$

where ρ_T and ρ_L are the transverse and longitudinal resistivity, respectively. ρ is the electrical resistivity of the Pt. $\Delta\rho_{Hall}B_z$ describes the change in resistivity caused by the ordinary Hall effect and $\Delta\rho_{add}B_z$ is the additional resistivity change on top of $\Delta\rho_{Hall}B_z$, as observed for saturated magnetic fields.[18] B_z is the magnetic field in the z-direction. m_x, m_y, and m_z are the components of the magnetization in the x-, y-, and z-direction, respectively, defined by $m_x = \cos\alpha\cos\beta$, $m_y = \sin\alpha\cos\beta$, and $m_z = \sin\beta$, where α is the in-plane angle between the applied field B and J_e, and β is the angle by which M is tilted out of the plane. For an applied field in the z-direction, from the Stoner-Wohlfarth model,[19] $\beta = \arcsin B/B_s$. $\Delta\rho_0$, $\Delta\rho_1$ and $\Delta\rho_2$ are resistivity changes as defined below[11]

$$\frac{\Delta\rho_0}{\rho} = -\theta_{SH}^2 \frac{2\lambda}{d_N}\tanh\frac{d_N}{2\lambda}, \quad (3)$$

$$\frac{\Delta\rho_1}{\rho} = \theta_{SH}^2 \frac{\lambda}{d_N}\mathrm{Re}\left(\frac{2\lambda G_{\uparrow\downarrow}\tanh^2\frac{d_N}{2\lambda}}{\sigma + 2\lambda G_{\uparrow\downarrow}\coth\frac{d_N}{\lambda}}\right), \quad (4)$$

$$\frac{\Delta\rho_2}{\rho} = -\theta_{SH}^2 \frac{\lambda}{d_N}\mathrm{Im}\left(\frac{2\lambda G_{\uparrow\downarrow}\tanh^2\frac{d_N}{2\lambda}}{\sigma + 2\lambda G_{\uparrow\downarrow}\coth\frac{d_N}{\lambda}}\right), \quad (5)$$

where θ_{SH}, λ, d_N, $G_{\uparrow\downarrow}$, and σ are the spin-Hall angle, the spin relaxation length, the Pt thickness, the spin-mixing conductance per unit area ($G_{\uparrow\downarrow} = G_r + iG_i$), and the bulk conductivity, respectively.

From Eq. (1), G_i is most dominant in the transverse configuration when the product $m_x m_y$ vanishes ($\Delta\rho_2$ is a function of G_i). This is the case for $\alpha = 0°$ and $\alpha = 90°$, as is shown in Fig. 1(a). As m_z scales linearly with B, the term $\Delta\rho_2 m_z$, contributes an additional linear dependence for $B < B_s$ that causes an offset between resistances for positive and negative saturation fields. This behaviour is clearly observed in the inset of Fig. 1(a), where the measurement for $\alpha = 90°$ is separately shown. For $\alpha = 45°$ (135°), the product $m_x m_y$ is maximized (minimized) and a maximum (minimum) change in resistance is observed.

These measurements were repeated for a set of samples with different Pt thicknesses [3, 4, 8, and 35 nm]. Results of the thickness dependent transverse resistance are shown in Fig. 2. For $\alpha = 45°$, at which both G_r and G_i contribute to a maximum SMR signal, a clear thickness dependence is observed at all field values. The thickness dependence of the slope $\Delta R_T/\Delta B$ at saturation fields is shown in the inset of Fig. 2, where the red dots represent the experiments. The black line (dots) shows the expected (observed) slope from the ordinary Hall effect (measured on a SiO_2/Pt sample) given by the equation $(\Delta R_T/\Delta B)_{Hall} = R_H/d_N$, where $R_H = -0.23 \times 10^{-10}\,\mathrm{m}^3/\mathrm{C}$ is the Hall coefficient of Pt.[20] $\Delta R_T/\Delta B$ for YIG/Pt behaves distinctively different. When decreasing

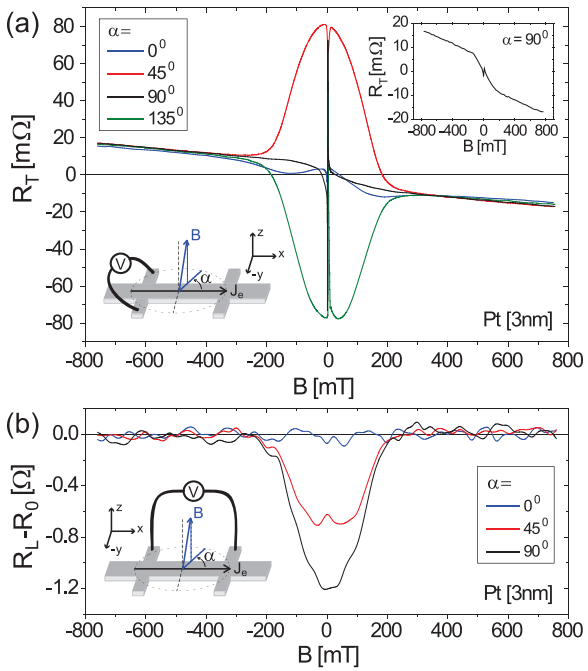

FIG. 1. (a) Transverse and (b) longitudinal resistance of Pt [3 nm] on YIG under an applied out-of-plane magnetic field. α is the angle between J_e and the small in-plane component of the applied magnetic field. The insets show the configuration of the measurements, as well as a separate plot of the transverse resistance for $\alpha = 90°$, where the contribution of G_i is most prominent. R_0 is the high-field resistance of the Pt film, here 1695 Ω.

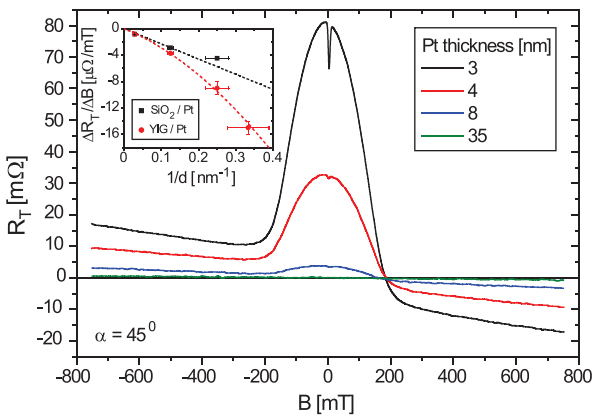

FIG. 2. Out-of-plane magnetic field sweeps on YIG/Pt for different Pt thicknesses [3, 4, 8, and 35nm], fixing $\alpha = 45°$. In the saturated regime ($B > B_s$), linear behaviour is observed. The inset shows the measured slope $\Delta R_T/\Delta B$ in the saturated regimes (red dots). The expected (black line) and measured (black dots) slopes for the ordinary Hall effect, on a SiO_2/Pt sample, are also displayed. The red dotted line is a guide for the eye.

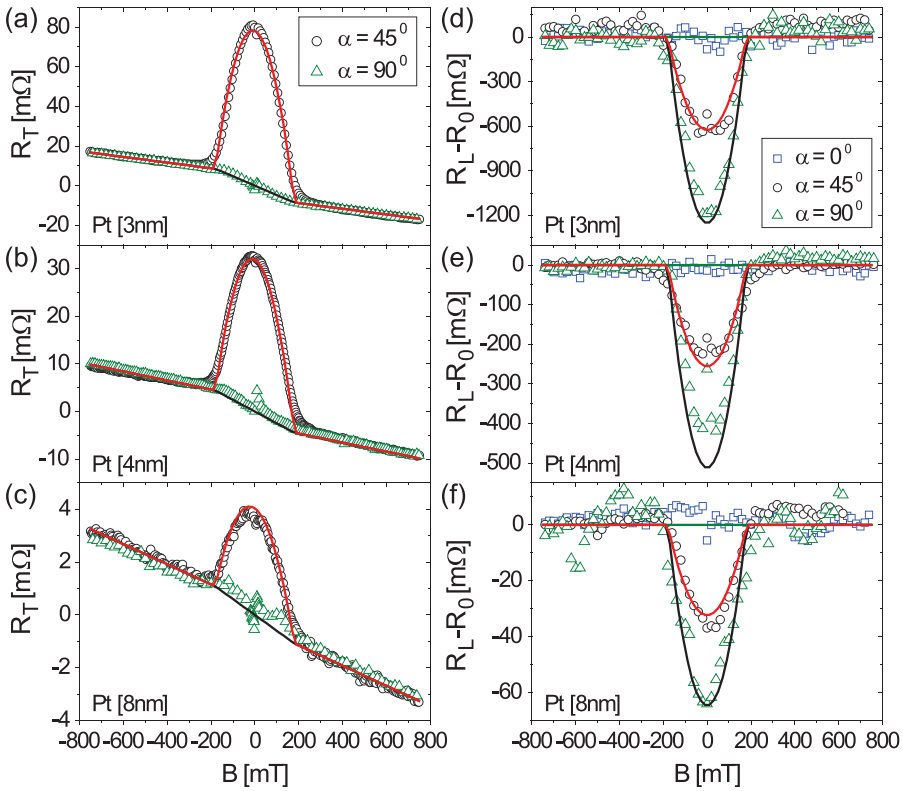

FIG. 3. Theory Eqs. (1) and (2) fitted (solid lines) to (a)–(c) transverse and (d)–(f) longitudinal observed resistances (open symbols) for different α and Pt thicknesses 3, 4, and 8 nm, respectively, using $\theta_{SH} = 0.08$, $\lambda = 1.2$ nm, $G_r = 4.4 \times 10^{14}\,\Omega^{-1}\,\mathrm{m}^{-2}$, and $G_i = 2.8 \times 10^{13}\,\Omega^{-1}\mathrm{m}^{-2}$. R_0 is the high-field longitudinal resistance of the Pt film of 1695 Ω, 930 Ω, and 290 Ω for the 3, 4, and 8 nm Pt thickness, respectively.

the Pt thickness, $\Delta R_T/\Delta B$ of YIG/Pt increases faster than expected from the ordinary Hall effect. This discrepancy cannot be explained by the present theory for the SMR and may thus indicate a different proximity effect. The red dotted line in the inset of Fig. 2 is a guide for the eye and represents the term $\Delta\rho_{Hall} + \Delta\rho_{add}$ in Eq. (1).

The SMR, including the resistance offset obtained by linear extrapolation of the high field regimes, is only significant for the thin Pt layers [3, 4, and 8 nm]. The thick Pt layer [35 nm] shows no (or very small) SMR.

Using Eqs. (1) and (2), all experimental data can be fitted simultaneously by the adjustable parameters θ_{SH}, λ, G_r, and G_i. $\rho = 1/\sigma$ follows from the measured resistances R_0 for each Pt thickness given in the caption of Fig. 3. The quality of the fit is demonstrated by Figs. 3(a)–3(f) for $\theta_{SH} = 0.08$, $\lambda = 1.2$ nm, $G_r = 4.4 \times 10^{14}\,\Omega^{-1}\mathrm{m}^{-2}$, and $G_i = 2.8 \times 10^{13}\,\Omega^{-1}\,\mathrm{m}^{-2}$. The measurements are very well described by the SMR theory (Eqs. (1) and (2)), for all Pt-thicknesses and magnetic field strength and direction. However, due to the correlation between the fitting parameters, similarly good fitting results can be obtained by other combinations of θ_{SH}, λ, G_r, and G_i, notwithstanding the good signal-to-noise-ratio of the experimental data. We therefore fixed the Hall angle at $\theta_{SH} = 0.08$, which is within the range 0.06–0.11 obtained from the fitting and consistent with results published by several groups.[12,21–24] By fixing θ_{SH}, the quality of the fits is not reduced, but the accuracy of the parameter estimations improves significantly. By Fig. 4, it is observed that a strong correlation exists between both G_r and G_i, and λ, whereas the ratio G_r/G_i does not significantly change (see inset Fig. 4). A good fit cannot be obtained for $\lambda > 1.4$ nm. For $\lambda < 0.8$ nm the error bars become very large and for $\lambda < 0.4$ nm a good fit can no longer be obtained. Inspecting Fig. 4, we favour $\lambda = 1.1 \pm 0.3$ nm, $G_r = (7 \pm 3) \times 10^{14}\,\Omega^{-1}\,\mathrm{m}^{-2}$, and $G_i = (5 \pm 3) \times 10^{13}\,\Omega^{-1}\,\mathrm{m}^{-2}$, where the higher values of G_r and G_i correspond to smaller λ. The ratio $G_r/G_i = 16 \pm 4$ does not depend on λ.

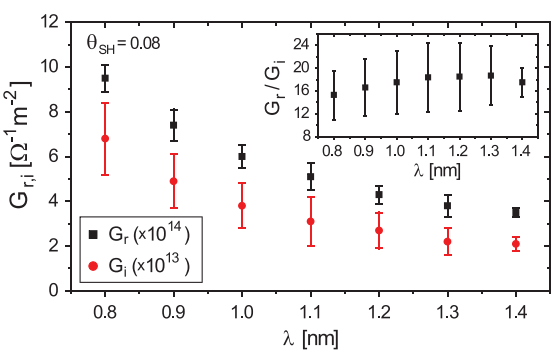

FIG. 4. Obtained magnitude and uncertainties of G_r and G_i (G_r/G_i in the inset) as a function of λ, for $\theta_{SH} = 0.08$.

In summary, by employing the SMR, including the contribution of the imaginary part of the spin-mixing conductance, it is possible to fully determine the magnetization direction of an insulating ferromagnetic layer, by purely electrical measurements. The experimental data are described well by the spin-diffusion model of the SMR, for all investigated Pt thicknesses and magnetic configurations. By fixing $\theta_{SH} = 0.08$, we find the parameters $\lambda = 1.1 \pm 0.3$ nm, $G_r = (7 \pm 3) \times 10^{14}\,\Omega^{-1}\,\mathrm{m}^{-2}$, $G_i = (5 \pm 3) \times 10^{13}\,\Omega^{-1}\mathrm{m}^{-2}$, and $G_r/G_i = 16 \pm 4$ for YIG/Pt bilayer structures.

We would like to acknowledge B. Wolfs, M. de Roosz, and J. G. Holstein for technical assistance. This work is part of the research program of the Foundation for Fundamental Research on Matter (FOM), EU-ICT-7 "MACALO," and DFG Priority Programme 1538 "Spin-Caloric Transport" (BA 2954/1-1) and is supported by NanoNextNL, a micro and nanotechnology consortium of the Government of the

Netherlands and 130 partners, by NanoLab NL, and the Zernike Institute for Advanced Materials.

[1]C. Burrowes, B. Heinrich, B. Kardasz, E. A. Montoya, E. Girt, Y. Sun, Y.-Y. Song, and M. Wu, Appl. Phys. Lett. **100**, 092403 (2012).
[2]Y. Tserkovnyak, A. Brataas, and G. E. W. Bauer, Phys. Rev. B **66**, 224403 (2002).
[3]Y. Kajiwara, S. Takahashi, S. Maekawa, and E. Saitoh, IEEE Trans. Magn. **47**, 1591 (2011).
[4]K. Xia, P. J. Kelly, G. E. W. Bauer, A. Brataas, and I. Turek, Phys. Rev. B **65**, 220401 (2002).
[5]D. Ralph and M. Stiles, J. Magn. Magn. Mater. **320**, 1190 (2008).
[6]Z. Wang, Y. Sun, Y.-Y. Song, M. Wu, H. Schultheiß, J. E. Pearson, and A. Hoffmann, Appl. Phys. Lett. **99**, 162511 (2011).
[7]Y. Kajiwara, K. Harii, S. Takahashi, J. Ohe, K. Uchida, M. Mizuguchi, H. Umezawa, H. Kawai, K. Ando, K. Takanashi, S. Maekawa, and E. Saitoh, Nature (London) **464**, 262 (2010).
[8]X. Jia, K. Liu, K. Xia, and G. E. W. Bauer, Europhys. Lett. **96**, 17005 (2011).
[9]F. D. Czeschka, L. Dreher, M. S. Brandt, M. Weiler, M. Althammer, I.-M. Imort, G. Reiss, A. Thomas, W. Schoch, W. Limmer, H. Huebl, R. Gross, and S. T. B. Goennenwein, Phys. Rev. Lett. **107**, 046601 (2011).
[10]V. Castel, N. Vlietstra, J. Ben Youssef, and B. J. van Wees, Appl. Phys. Lett. **101**, 132414 (2012).
[11]Y.-T. Chen, S. Takahashi, H. Nakayama, M. Althammer, S. T. B. Goennenwein, E. Saitoh, and G. E. W. Bauer, Phys. Rev. B **87**, 144411 (2013).
[12]N. Vlietstra, J. Shan, V. Castel, B. J. van Wees, and J. Ben Youssef, Phys. Rev. B **87**, 184421 (2013).
[13]H. Nakayama, M. Althammer, Y.-T. Chen, K. Uchida, Y. Kajiwara, D. Kikuchi, T. Ohtani, S. Geprägs, M. Opel, S. Takahashi, R. Gross, G. E. W. Bauer, S. T. B. Goennenwein, and E. Saitoh, Phys. Rev. Lett. **110**, 206601 (2013).
[14]C. Hahn, G. de Loubens, O. Klein, M. Viret, V. V. Naletov, and J. Ben Youssef, Phys. Rev. B **87**, 174417 (2013).
[15]M. Althammer, S. Meyer, H. Nakayama, M. Schreier, S. Altmannshofer, M. Weiler, H. Huebl, S. Geprägs, M. Opel, R. Gross, D. Meier, C. Klewe, T. Kuschel, J.-M. Schmalhorst, G. Reiss, L. Shen, A. Gupta, Y.-T. Chen, G. E. W. Bauer, E. Saitoh, and S. T. B. Goennenwein, Phys. Rev. B **87**, 224401 (2013).
[16]The authors of Ref. 15 obtained G_i by adding the saturation magnetization to the applied magnetic field to obtain the total magnetic field in the Pt. In our opinion, the saturation magnetization should not be included, which leads to a different zero-field extrapolation resulting in $G_i = 1.7 \times 10^{13}\,\Omega^{-1}\,\mathrm{m}^{-2}$, which is more close to the uncertainty interval of our results.
[17]V. Castel, N. Vlietstra, B. J. van Wees, and J. Ben Youssef, Phys. Rev. B **86**, 134419 (2012).
[18]From the measurements for $\alpha = 90°$, shown in the inset of Fig. 1(a) and in Figs. 3(a)–3(c), we deduce that also in the non-saturated regime, this additional effect likely scales linearly with B. The dominant linear effect observed in the non-saturated regime is attributed to G_i. The remaining linear signal is explained by the sum of the ordinary hall effect and the additional term as defined in Eq. (1).
[19]E. Stoner and E. Wohlfarth, IEEE Trans. Magn. **27**, 3475 (1991).
[20]C. M. Hurd, *The Hall Effect in Metals and Alloys* (Plenum Press, New York, 1972).
[21]L. Liu, R. A. Buhrman, and D. C. Ralph, e-print arXiv:1111.3702v3 [cond-mat.mes-hall].
[22]L. Liu, T. Moriyama, D. C. Ralph, and R. A. Buhrman, Phys. Rev. Lett. **106**, 036601 (2011).
[23]K. Ando, S. Takahashi, K. Harii, K. Sasage, J. Ieda, S. Maekawa, and E. Saitoh, Phys. Rev. Lett. **101**, 036601 (2008).
[24]A. Azevedo, L. H. Vilela-Leão, R. L. Rodríguez-Suárez, A. F. Lacerda Santos, and S. M. Rezende, Phys. Rev. B **83**, 144402 (2011).